Geochemical News 140 | Jul 2009

In This Issue

GNews 140 Staff

Stephen Komor, Ph.D. (Editor)
U.S. Geological Society (retired)
sck15@cornell.edu

Thilo Behrends, Ph.D.
Utrecht University

Bhoopesh Mishra, Ph.D.
Princeton University

Mitch Schulte, Ph.D.
University of Missouri - Columbia

Angie Souren, M.Sc.
SmarterScience

The Universal Stage: The Past, Present, and Future of a Mineralogical Research Instrument

by Daniel E. Kile
Scientist Emeritus, U.S. Geological Survey, Denver, Colorado
Adjunct Instructor, College of Microscopy, Westmont, Illinois

Introduction

The optical behavior in crystals (with the exception of those crystallizing in the cubic system) varies with the direction of light travel within the crystal, and measurement of optical properties has to be carried out in specific orientations. Therefore a great variety of rotating devices have been designed to align crystals into a proper orientation. The universal stage is certainly the most important of such devices, and for more than half a century it was considered essential for petrographic work.

One of the most elegant of all accessories for the petrographic microscope, the universal stage could be regarded as an elaborate crystallographic goniometer, the only difference from traditional goniometers being that *optical*, in addition to geometric features, can be measured. Named for its capability for angular measurements in both horizontal and vertical planes, it is an intricate device that consists of concentric, graduated rings that can be tilted (via gimbals) and rotated, which, in addition to folding, graduated Wright arcs, permit quantification of the angular movement of multiple axes. This device was designed to be used primarily with thin sections (i.e., rock sections that are mounted on a glass slide and cut to a thickness of 0.03 mm), whereby a sample is positioned on the stage between glass hemispheres (also known as segments) using glycerin as a mounting fluid; this arrangement allows light to pass unobstructed through the mineral grain without deviation by reflection when the stage is tilted to high angles. Thus, planar features such as twin planes, cleavage, and principal optical directions can be located, giving details of the relation between optical and crystallographic orientation on a sample that cannot be obtained in any other way. Unfortunately, because of increasing reliance on computer-driven microbeam instruments, use of the universal stage has decreased in past years, despite its irreplaceable utility.

Construction of the 4-Axis Universal Stage

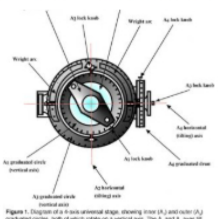

Figure 1

Universal stages have been developed with two, three, four, or five axes; these axes have been described by a variety of nomenclatures, but one of the most convenient is that proposed by Berek (1924), whereby the axes are numbered sequentially from innermost to outermost, i.e., from A_1 to A_5 for a five-axis stage (the stage of the microscope itself would constitute a sixth axis). Of the above options, it is the 4-axis stage that has proven to be the most commonly manufactured and used, despite that the third, A_3 axis (the outer rotating graduated circle, vertical axis), is seldom required for routine measurement. Thus, in practice, only three axes are essential: two inner axes, designated as A_1 (the inner rotating graduated circle, vertical axis) and A_2 (the inner horizontal tilting axis), and one outer tilting horizontal axis, the A_4 (see figure 1), which is controlled by a large graduated vertical drum on the right side of the stage. Two hinged Wright arcs, used to measure the tilt of the A_2 axis, are provided in most versions of the universal stage, although some manufacturers substituted a graduated protractor in place of the Wright arcs; the arcs are normally folded down when not needed. The angular movement of each axis can be quantified: rotation of the A_1 and A_3 axes are read from the 360° scales on their rings, the tilt of the A_2 axis is read from graduations on one of the folding Wright arcs, and the tilt of the A_4 axis is measured from a vernier scale on the vertical drum. Each axis also has its own locking device to fix it in place as needed during manipulation. Most stages have a center glass plate that is set into a threaded ring, which is used to adjust the height of a slide. The entire stage is attached, via solid uprights, to a base plate with a large central aperture; the plate is drilled to fit the microscope stage using two threaded screws; more modern universal stages feature an x-y centerable base plate that is attached to the microscope stage, which facilitates adjustment. Variations to this general design are described in more detail below.

Historical Development and Design

Figure 2

E.S. Fedorov developed a four-axis universal stage in 1892 (Fedorov, 1892, 1894) in response to a need to characterize feldspar-group minerals (figure 2). By the late 1800s, classification and petrological interpretation of rocks had become increasingly important, and this required the identification of the feldspars, which constitute a major group of the rock-forming minerals. Identification of the plagioclase feldspars was based on the relation between the principal optical vibration directions (*X, Y, Z*) and crystal twin planes (albite, pericline, Carlsbad, and Carlsbad-albite) of a mineral grain, from which its chemical composition could be determined. Fedorov's universal stage, with independently tilting and rotating axes, facilitated these measurements by allowing complete freedom to orient crystallographic and optical planes of the sample to vertical, north-south positions, which can then be plotted (as east-west horizontal poles) on a Wulff stereonet to assess angular relations between the planes.

One drawback of the early Fedorov stage, however, was its small size (the outer ring is only about 7 cm in diameter), which rendered it difficult to manipulate. These stages required use of circular, 2-cm diameter thin sections that were prepared without a coverslip; such preparations were oriented on the stage with the rock section facing down (Medenbach, 2008) in order to ensure its proper height within the glass segments. Moreover, the earliest form of the Fedorov stage provided no means of measuring the tilt of the inner horizontal axis, but

Figure 3

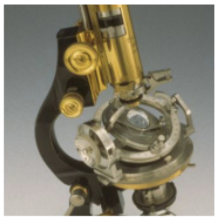

Figure 4

Figure 5

Figure 6

provided no means of measuring the tilt of the inner horizontal axis, but by 1911, F.E. Wright had introduced graduated, folding arcs (which now bear his name) that permitted quantitative angular measurement from the innermost tilting graduated circle.

A larger-format stage was introduced in 1912, as an integral part of a large theodolite microscope, by the firm of R. Fuess, Berlin-Steglitz (Leiss, 1912; Fuess, 1919); this instrument was later manufactured also by C. Leiss, Berlin-Steglitz (figure 3; see also Leiss, 1925). This stage was an important improvement in that, rather than being constrained by the small and unwieldy circular slides required by the Fedorov stage, it allowed use of a standard size (ca. 25 x 45 mm) thin section. In addition to its universal stage, the theodolite microscope features a slotted Wright universal eyepiece and synchronous rotation of analyzer and polarizer; it is thus one of the most complex mineralogical microscopes ever made. Accordingly, a significant drawback to this instrument was its high cost - which was on the order of the annual salary of the company's chief mechanic.

The issue of cost was mitigated by Max Berek, who designed a large-format detachable 4-axis universal stage in the early 1920s (figure 4), which was introduced by the firm of E. Leitz (Berek, 1924); this stage could easily be attached to most of the petrographic microscopes of the era. Although there are numerous variations of this pattern by different makers, Berek's design (described in the preceding section) is the general form, essentially unchanged to the present day (figure 5), which was manufactured by numerous instrument makers through the 1980s. Nonetheless, some modifications are evident among the various firms; for example, each company fabricated their hemispheres with a differing size and configuration of the metal frame. Most makers, including Leitz and Bausch & Lomb, incorporated a removable center glass plate, but others, such as Zeiss, used a drop-in lower hemisphere that eliminated the necessity for this center glass.

Though the 4-axis stage is by far the most common, alternative ideas appeared early. A 5-axis universal stage was developed in 1929 by R.C. Emmons at the University of Wisconsin (Emmons, 1929a). This design (figure 6) featured an additional ring between the A_1 and A_3 graduated circles, and a second set of Wright arcs; it had some advantages in that it simplified stereonet plotting, but has otherwise fallen into disuse because of its greater complexity, reduced stability, and higher cost. By the early 1950s, a 3-axis stage was introduced by the English firm of Cooke, Troughton & Simms in recognition of the fact that fewer axes equate to greater stability and simplified operation, and that only three axes are necessary for almost all required measurements; Rathenow Optical Works in Germany manufactured their own version of a 3-axis stage in the 1960s. However, this innovative design, like the 5-axis, never attained a high level of popularity. A further variant is the 2-axis stage, manufactured by E. Leitz; designated the UT-2, this stage has only the A_1 and A_4 axes; Wright arcs, unnecessary in the absence of a tilting A_2 axis, are absent. This seldom-seen stage was intended primarily for classroom instruction or for use with a universal stage ¬refractometer.

Principles of Universal Stage Measurement

The optical data of any mineral are in general very sensitive to changes in chemical and physical conditions during their formation, and thus may be excellent petrogenetic indicators. As many as five different optical values can be measured in birefringent crystals, which are subdivided into uniaxial (one optic axis) and biaxial (two optic axes) groups (e.g., see Nesse, 2004; Dyar et al., 2008). These are the principal indices of refraction (which correspond to a principal vibration direction; there are two for uniaxial minerals in the tetragonal and hexagonal systems, and three for biaxial minerals in the orthorhombic, monoclinic, and triclinic systems), the optic axial angle (2V), and in monoclinic and triclinic crystals, the orientation of the principal indices of refraction with respect to the crystallographic axes. The universal stage, with its capability for multi-axis orientation of a crystal grain, is well suited for the determination of the axial angle (2V) and the assessment of crystal optics (i.e., principal vibration directions, designated *X, Y, Z*) relative to crystallographic axes (designated a, b, c). The principal indices of refraction can also be measured with good accuracy using specialized equipment (see following section).

Minerals in the tetragonal and orthorhombic crystal systems have three crystallographic axes that are mutually perpendicular, and hexagonal minerals have four axes, three of which are at 60° to each other and perpendicular to the c-axis. Optical directions (i.e., principal vibration directions) must always be mutually perpendicular. Thus, for tetragonal and hexagonal minerals, one optical direction is parallel to the c axis and the other lies in a plane perpendicular to it. For orthorhombic minerals, all three optical directions coincide with crystallographic axes. However, for lower symmetries, crystallographic axes are not all mutually perpendicular. For example, in the case of monoclinic minerals (the most common symmetry in naturally occurring species), the angle between the crystallographic a- and c- axes is different from 90°. Thus, for these symmetries, only the b-axis coincides with an optical direction, and the other two axes are related to optical directions by an angle other than 90°. In the case of triclinic minerals, none of the crystallographic axes correspond to any optical direction.

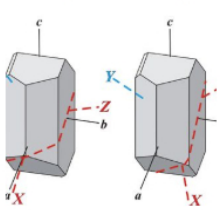

Figure 7

Knowledge of the angular relation between crystallographic and optical axes is important because this relation changes with compositional substitution throughout a solid-solution series of minerals, for example, such as seen with the plagioclase feldspars (figure 7). When optical and crystallographic orientation data for the plagioclase feldspars are compared to well-established diagrams showing the relation of these data to composition (e.g., see Tröger et al., 1979, or Burri et al., 1967), an accuracy to ± 2% or better can be quickly and easily attained.

Further information on the use of the universal stage is given in Berek, 1924; Reinhard, 1931; Nikitin, 1936; Haff, 1940, 1942; Emmons, 1943; Naidu, 1958; Slemmons, 1970; Phillips, 1971; and Muir, 1981.

Utility of the Universal Stage, Past and Present

The universal stage was originally designed for work with the plagioclase feldspars, and indeed it is still effective for that task, but in recent decades it has been supplanted by microprobe analysis (e.g., see Kile, 2006). In contrast to microbeam instruments, however, the universal stage remains much more affordable, permits a much quicker analysis, and provides accuracy at least as high as that of the microprobe. The major drawback to using the universal stage is that using it requires a specialized knowledge, which is becoming increasingly difficult to acquire as those proficient in its operation are rapidly dwindling in number.

Some earlier as well as more contemporary applications for the universal stage include:

1. Assessment of the fabric and deformation-recrystallization history of metamorphic rocks by determining the orientation of the c-axis in quartz grains in thin section (e.g., see Fairbairn, 1949).

2. Identification of plagioclase feldspar crystals based on the relation between crystallographic planes (i.e., twin planes) and optic orientation (i.e., principal vibration directions), which in turn provides chemistry (e.g., Reinhard, 1931; Tröger et al., 1979). Additionally, an analysis of Si/Al order/disorder of sanidine-orthoclase crystals, based on an assessment of the optic orientation relative to the Carlsbad twin plane and measurement of the optic angle, can provide information on the cooling history of the crystals (e.g., see Su, 1984).
3. Identification of minerals in thin section (especially for thin sections with cover slips that cannot be analyzed with a microprobe) by determining relations between crystallographic directions (i.e., cleavage planes and zone axes) and optic vibration directions, quantitative measurement of optic angle, characterization of extinction angles (i.e., Z-to-c), and determination of birefringence using a Berek compensator. For example, measurement of the optic angle (2V) for minerals in the olivine group can distinguish among species in a solid-solution series from Mg-rich forsterite to Fe-rich fayalite (e.g., see Nesse, 2004 and references therein).
4. Evaluation of twinning in mineral fragments and identification of twin laws (e.g., normal, parallel, or complex twins; see Phillips, 1971). Minerals often studied include those in the plagioclase, pyroxene, and amphibole groups.
5. Measurement of refractive index in grains. With specialized equipment (such as proposed by Wilcox, 1959), including an Emmons cell for temperature control, refractive indices can be rapidly determined with a 'double variation' method, whereby both temperature and wavelength can be varied such that a match in the index of a mineral grain and an index liquid can be attained with a minimal changing of index liquids (Emmons, 1928, 1929b). This procedure has not seen much use since the early 1960s with the universal stage, but has been used in recent years with the spindle stage (e.g., Medenbach, 1985).
6. Assessment of meteorite impact sites by determining the relation between crystallographic orientation (i.e., c-axis orientation) and shock-induced planar deformation features in quartz (e.g., see Stöffler and Langenhorst, 1994; Grieve et al., 1996; and Ellwood et al., 2003).
7. Measurement of extinction angles (e.g., Z-to-c) in pyroxene- and amphibole-group minerals (Haff, 1941; Turner, 1942) can aid in the identification the species within a group (e.g., Winchell, 1951).
8. Measurement of dihedral angles of crystal grain boundaries in thin sections to evaluate crystallization and other magmatic processes in igneous rocks (e.g., Holness, 2005; Holness et al., 2005, 2007).

It is of note that many of the measurements described above cannot be done by any other method.

Abbreviated Procedure for Universal Stage Manipulation

Although a complete understanding of the function of the universal stage, in context with the fundamentals of mineral optics, requires considerable practice, the basic elements of its manipulation are straightforward. The universal stage is used with two hemispheres whose refractive indices are selected to approximately match the mineral being examined (usually in thin section, but grain mounts can also be used in special preparations). The sample is mounted between glass hemispheres (glycerin is often used because it is water-soluble, greatly simplifying instrument cleanup), which, in conjunction with a center glass and the thin section, constitute a sphere, allowing an axis to be tilted without exceeding the critical angle for reflection at an air interface. The basics of operation entail orienting either a crystallographic plane (cleavage or twin) or a principal optical plane (*X-Y*, *X-Z*, or *Y-Z*) to a vertical and north-south position, whereby its pole will be horizontal and east-west.

Before work can begin, the stage must be properly aligned. A detailed description of this procedure is beyond the scope of this paper, but in brief, a series of steps are carried out to ensure that the grain being examined is in the exact center of the sphere (formed by the hemispheres, slide, and center plate), that the vertical axes are coaxial with the optical axis of the microscope (i.e., centered to the microscope stage), and that both horizontal axes are exactly parallel to an eyepiece cross hair, such that when an axis is tilted, a particle in the field of view travels exactly north-south or east-west.

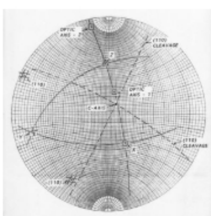

Figure 8

Orientation of cleavage planes is a relatively simple operation: the inner vertical (A_1) axis, is rotated, and the inner horizontal (A_2) axis is tilted in an alternating manner such that the plane is vertical and north-south, evidenced by a sharp line in plane polarized light. Its pole, now oriented horizontal and east-west, is then plotted on a stereonet based on the angular readings taken from the A_1 and A_2 axes. The Wulff stereographic net, introduced in 1902, is used for plotting (e.g., Haff, 1940); it is a circular grid from which angular relations of objects plotted in two dimensions can be determined in three dimensions (figure 8).

Orientation of optic planes is somewhat more difficult. The mineral is oriented by sequentially rotating the inner vertical (A_1) axis, and tilting the inner horizontal (A_2) axis, in an alternating fashion such that the mineral is brought to extinction, and remains at extinction when the outer horizontal axis (A_4) is turned (thus tilting the entire stage on an east-west axis). The plane is now vertical and north-south. If one of the planes thus oriented (north-south) contains an optic axis, it can readily be located by rotating the microscope stage (designated A_5) counterclockwise 45° and tilting the horizontal A_4 axis to a point where the grain is dark (this is a point of optic axis zero retardation, seen when the optic axis is vertical to the microscope stage); an optic axis position (vs. an extinction position) is confirmed if the grain remains dark with complete rotation of the microscope stage (A_5). Two principal vibration directions can always be directly located from these measurements, and the position of the third is established geometrically on the stereonet plot, which is unambiguous since all poles must be mutually 90° apart.
The above protocol allows for a very complete evaluation of the mineral. Cleavage angles, zone axes, optic axes, and their relation to the principal vibration directions are now known, giving a detailed knowledge of the relation between the crystallographic axes and principal optic directions (see accompanying diagram). No other method exists to completely characterize the optical and crystallographic properties of a mineral in thin section!

Equipment for the Universal Stage

Leitz equipment will be mostly described in this section, inasmuch as these stages and accessories are most often available on the surplus science instrument market; they are also readily adaptable to a wider range of microscope.

Two kinds of observation are possible with the universal stage. The universal stage is generally used orthoscopically, with special long-working-distance objectives of relatively low magnification. However, it can also be used conoscopically (i.e., for observation of interference figures), using objectives of higher magnification in conjunction with smaller-diameter hemispheres (which accommodate shorter objective working distances) and either a special dedicated high-numerical-aperture conoscopic condenser, or a normal polarizing condenser to which a conoscopic top element is attached. Additional details are provided below in this section.

Hemispheres
Universal stage hemisphere glass is typically provided (as by E. Leitz) in three refractive indices: 1.516, 1.554, and 1.649. These indices are intended to approximately match those of minerals from one of three major groups (K-feldspar, quartz-plagioclase, or pyroxene-amphibole, respectively), which minimizes deviation in the light path between the glass and the mineral. In addition to the large-diameter orthoscopic segments, conoscopic hemispheres of the same refractive indices with smaller diameters were manufactured to accommodate the shorter working distance of the higher numerical aperture conoscopic objectives used with them. Additionally, specially modified metal frames for the upper hemispheres were offered with a trackway that permitted use of a graduated Schmidt guide; this arrangement provided a calibrated parallel displacement of a slide, used for petrofabric and structural

analyses of thin sections. Considering that the firm of E. Leitz manufactured both orthoscopic and conoscopic upper hemispheres in three refractive indices, in addition to the modification for the Schmidt guide, a total of 12 distinct upper hemispheres were marketed by Leitz for use with their universal stage. High-index hemispheres (e.g., n_D = 1.71) were also available by special order.

Objectives
Because of the thickness of the glass hemispheres, special long-working-distance objectives are required in order to focus on the slide. These objectives also must have an internal iris diaphragm that provides parallel (i.e., orthoscopic) illumination, which is essential for the accurate setting of a mineral to extinction; alternatively, Zeiss provided fixed-diaphragm inserts that were placed inside the objectives. It should be noted that the resolution (i.e., numerical aperture) of long- working-distance objectives is greatly diminished compared to that of a normal objective; this becomes even more readily apparent when the internal diaphragm is partially stopped down. Manufacturers provided several magnifications for work in orthoscopic illumination, e.g., 5, 10, 20, and 32x. Objectives for conoscopic examination were provided by Leitz in magnifications of 32 and 50x.

Condensers and condenser top elements
Orthoscopic observation requires only the normal polarizing condenser, although special condenser top elements were available for this purpose. Work at higher magnifications or conoscopic observation necessitates the use of converging light, provided by either an auxiliary condenser top lens element, or a dedicated high-numerical-aperture condenser (Zeiss also provided a high-numerical-aperture 'UD' condenser for this purpose). The firm of E. Leitz provided a bewildering variety of such top elements to fit different generations of condenser design, each with different optics and thread sizes.

In summary, altogether the firm of E. Leitz in the 1970s manufactured six long-working-distance objectives (three orthoscopic and two conoscopic, not counting a special low-magnification centering objective), a variety of condensers and top elements to fit different condenser types, three lower hemispheres (n_D = 1.515, 1.554, and 1.649), and 12 different upper hemispheres. The above totals do not include hemispheres that could be special ordered, such as high-index hemispheres, typically manufactured in indices around n_D = 1.72. Needless to say, the use of the universal stage in an earlier era warranted manufacture of all manner of accessories to accommodate them.

Accessories for the Universal Stage

A variety of accessories were developed for the universal stage, which extend its capability throughout a wide range of observation; a few are briefly described below. Further details are given in Kile (2003) and references therein.

Waldmann hollow sphere

Figure 9

The Waldmann hollow sphere, manufactured by E. Leitz (figure 9), allows examination of mineral fragments or small gemstones that are immersed in an index liquid within the sphere. The specimen is mounted on a fitted holder, which then is inserted into a hollow glass sphere (25-mm diameter) which is filled with an index liquid; it is then placed in a special holder in the center of a universal stage. This arrangement permits almost unlimited rotation and orientation of a mineral grain or faceted gemstone for optical study.

Emmons cell
An Emmons cell consists of a circular hollow metal frame that holds a central glass plate and an integral lower hemisphere; it is temperature-controlled with circulating water, and used in the double variation method of refractive index determination for mineral grains, in which wavelength and temperature are both varied. Because the index of refraction for a liquid is inversely proportional to both temperature and wavelength, changing these variables (in conjunction with the ability to orient the mineral on the universal stage) greatly expedites the refractive index determination of a mineral by minimizing the necessity of changing calibrated liquids to achieve a match in index (i.e., no relief) with the mineral.

Berek compensator
Use of a Berek compensator in conjunction with a universal stage affords a powerful and expedient means of quantitatively measuring the retardation, from which birefringence (i.e., the mathematical difference in the high and low indices of refraction) of a mineral can be calculated. The compensator, which is inserted into the accessory slot above the nosepiece of the microscope, consists of a calcite plate approximately 0.1-mm thick, or, in more recently manufactured instruments, a magnesium fluoride plate. These plates, cut perpendicular to the c-axis, are mounted in a tilting frame that is connected to a geared drive mechanism and a graduated drum and vernier scale for measurement of rotation. This compensator was developed by Max Berek in 1913 (Berek, 1913), and its design had not appreciably changed for more than 60 years.

Tilting the compensator plate, when superimposed over an appropriately oriented mineral grain, will vary the degree of compensation until a point is reached when the compensator brings the grain to a point of zero retardation. A suitable grain is one whose optic axis (or optic plane) is parallel to the microscope stage in a 'subtractive' position relative to the compensator plate, i.e., the grain is oriented with its slow ray parallel to the fast ray of the plate. Attaining this orientation is greatly facilitated with the universal stage because of its multi-axis construction. Once compensation is achieved, a reading is taken from the drum of the compensator, and retardation is calculated. Birefringence is then calculated based on the measured retardation and a known grain thickness (the latter of which is dependent on the degree of tilt of the universal stage, and which can be determined from a simple trigonometric calculation).

Wright eyepiece
The Wright universal eyepiece, described by F. E. Wright in 1911, is used primarily for quantifying birefringence using a graduated quartz wedge, or to accurately set extinction positions, such as would be necessary to measure extinction angles. This instrument consists of a slotted eyepiece and cap analyzer that replace the regular cross hair eyepiece; the slot, located below the analyzer, is designed to accept a variety of specialized compensators. Two plates can be used to set extinction; these are the half-shade plate after Nakamura and the half-shade wedge after Macé de Lépinay. Both plates are composed of two parallel quartz sections, right- and left-handed, oriented in opposite directions. When one of these plates is superimposed over a grain, the precise setting of extinction is evidenced when the light intensity is perfectly balanced between both halves of the plate.

The Present and Future of the Universal Stage

With Zeiss having recently (1999) discontinued production of their universal stage (Leitz and Nikon had discontinued manufacture of their universal stages in the mid-1990s), there is currently no worldwide production of them. Used instruments are sometimes available, some of which may be in as new condition, but others of which can be in an unusable condition.

Moreover, petrographic microscopes capable of accommodating a universal stage, i.e., those with adequate stage clearance and a removable center stage plate to allow for freedom of tilting the outer A_4 axis, are no longer manufactured. Despite the fact that no modern manufacturer provides a microscope that will directly accommodate the universal stage, it is possible to adapt at least the Olympus BX-51P polarized light microscope, and perhaps other recently manufactured microscopes as well, to accommodate the universal stage (figure 10). In

Figure 10

microscopes as well, to accommodate the universal stage (figure 10). In the case of the Olympus microscope, a removable stage center plate is present, but a riser block needed to be fitted to achieve adequate stage clearance, and a stage intermediate adapter had to be fabricated that fit the universal stage mounting screws and allowed the assembly to be attached to the microscope stage (Delly, 2007).

Despite the fact that the last list price, in the mid-1990s, for a Leitz 4-axis stage with three sets of hemispheres was quite high, about $12,500, the cost of a modern microbeam instrument greatly exceeds that figure by more than an order of magnitude, with annual maintenance expenses being equally high. Thus given the comparative expense of a universal stage (including the cost of a polarized light microscope), the polarized light equipment is far more cost effective. Furthermore, most professionals in the working world will find that there is not a microprobe down the corridor, and contracting analytical work for x-ray diffraction and microbeam analysis can be both expensive and time consuming. However, the principal drawback to the petrographic microscope and universal stage, as mentioned earlier, is the effort required to learn the underlying principles and become proficient; well-grounded training in optical mineralogy takes a substantial investment of time and considerable practice that may take some years. In contrast, for the case of an x-ray diffractometer, a technician can be trained to prepare samples, operate the instrument, and generate a list of mineral phases present in about an hour (taking note that there is a strong possibility that the phases so identified - the result of a computer database search - may be incorrect).

Although some consider the universal stage to be obsolete, suggesting that it (along with polarized light microscopy in general) has been replaced by modern microbeam or x-ray diffraction instrumentation, the bottom line is that this equipment is a valuable adjunct to modern instrumental methods of analysis, as *nothing* can replace a trained human eye to interpret and evaluate the physical features of the sample and assess the veracity of computer-generated data (see Kile, 2006, for a further discussion of some of these issues). Thus, while there is no question that these modern computer-driven devices are extremely effective, they do *not* replace the light microscope. In the case of the universal stage, a declining number of professionals having a specialized knowledge (such methods are no longer taught at universities in the U.S.), and an increasing scarcity of equipment, will likely mandate its extinction, if for no other reason than no one will realize its capabilities; unfortunately, the outcome will be the loss of the irreplaceable utility of this instrument.

References

Berek, M. (1913) Zur Messung der Doppelbrechung hauptsächlich mit Hilfe des Polarisationsmikroskops. *Centralblatt für Mineralogie, Geologie und Paläontologie*, pp. 388-396, 427-435, 464-470.

Berek, M. (1924) *Mikroskopische Mineralbestimmung mit Hilfe der Universaldrehtischmethoden*. Gebrüder Borntraeger, Berlin, 168 p.

Burri, C., Parker, R.L., and Wenk, E. (1967) *Die optische Orientierung der Plagioklase*. Birkhäuser Verlag, Basel, Stuttgart, 334 p.

Delly, J.G. (2007) Universal stage use on the Olympus BX-51-pol microscope. http://www.modernmicroscopy.com

Dyar, M.D., Gunter, M.E., and Tasa, D. (2008) *Mineralogy and Optical Mineralogy*. Mineralogical Society of America, Chantilly, Virginia, 708 p.

Ellwood, B.B., Benoist, S.L., El Hassani, A., Wheeler, C., and Crick, R.E. (2003) Impact ejecta layer from the Mid-Devonian: Possible connection to global mass extinctions. *Science*, 300, 1734-1737.

Emmons, R.C. (1928) The double dispersion method of mineral determination. *The American Mineralogist*, **13**, 504-515.

Emmons, R.C. (1929a) A modified universal stage. *The American Mineralogist*, **14**, 441-461.

Emmons, R.C. (1929b) The double variation method of refractive index determination (second paper). *The American Mineralogist*, **14**, 414-426.

Emmons, R.C. (1943) The Universal Stage, with Five Axes of Rotation. *Geological Society of America Memoir* **8**, 205 p.

Fairbairn, H.W. (1949) *Structural Petrology of Deformed Rocks*. Addison-Wesley Publishing Co., Cambridge, 344 p.

Fedorov, E.S. (1892) Eine neue Methode der optischen Untersuchung von Krystallplatten in parallelem Lichte. *Tschermak's Mineralogische und Petrographische Mittheilungen* (for the year 1891), **12**, 505-509.

Fedorov, E.S. (1894) Universal- (Theodolith-) Methode in der Mineralogie und Petrographie. *Zeitschrift für Kristallographie und Mineralogie*, **22**, 229-268.

Fuess, R. (1919) Mineralogische und krystallographische In¬stru¬mente und Hilfs-Apparate; Katalog 180. E. Mikroskope für Mineralogie und physikalische Studien. R. Fuess mechanisch-optische Werkstätten, Berlin-Steglitz, p. 57-107.

Grieve, R.A.F., Langenhorst, F., and Stöffler, D. (1996) Shock metamorphism of quartz in nature and experiment: II. Significance in geoscience. *Meteoritics & Planetary Science*, **31**, 6-35.

Haff, J.C. (1940) Use of the Wulff net in mineral determination with the universal stage. *American Mineralogist*, **24**, 689-707.

Haff, J.C. (1941) Determination of extinction angles in augite and hornblende with the universal stage according to the method of Conrad Burri. *American Journal of Science*, **239**, 489-492.

Haff, J.C. (1942) Fedorow method (universal-stage) of indicatrix orientation. *Colorado School of Mines Quarterly*, **37**, 3-28.

Holness, M. (2005) Petrographic clues to overturn and eruption of open-system magma chambers: Santorini, Greece. In Abstracts of the 15th Annual V.M. Goldschmidt Conference, Moscow, Idaho, May 2005. *Geochimica et Cosmochimica Acta*, **69**, A-147.

Holness, M.B., Cheadle, M.J., and McKenzie, D. (2005) On the use of changes in dihedral angle to decode late-stage textural evolution in cumulates. *Journal of Petrology*, **46**, 1565-1583.

Holness, M.B., Nielson, T.F.D., and Tegner, C. (2007) Textural maturity of cumulates: A record of chamber filling, liquidus assemblage, cooling rate and large-scale convection in mafic layered intrusions. *Journal of Petrology*, **48**, 141-157.

Kile, D.E. (2003) *The Petrographic Microscope: Evolution of a Mineralogical Research Instrument*. Special Publication No. 1, Mineralogical Record Inc., Tucson, Arizona, 96 p.

Kile, D.E. (2006) Polarized light microscopy in geoscience education: Relevant or obsolete? *Elements* **2**, August 2006, 197-198.

Leiss, C. (1912) Neues petrographisches Mikroskop für die Theodolite-Methode. *Centralblatt für Mineralogie, Geologie und Paläontologie*, 733-736.

Leiss, C. (1925) *Die modernen optischen Messinstrumente des Kristallographen und Petrographen; ihre*

Beschreibung und Justierung. Verlag von Gustav Fischer, Jena, 91 p.

Medenbach, O. (1985) A new microrefractometer spindle-stage and its application. *Fortschritte der Mineralogie*, **63**, 111-133.

Medenbach, O. (2008) On antique crystal rotating apparatus and requirements regarding samples and their preparation. *Journal of the Microscope Historical Society*, **16**, 76-83.

Muir, I.D. (1981) *The 4-Axis Universal Stage*. Microscope Publications, Ltd., Chicago, 145 p.

Naidu, P.R.J. (1958) *4-Axes Universal Stage*. Commercial Printing & Publishing House, Madras, 106 p.

Nesse, W.D. (2004) *Introduction to Optical Mineralogy*, 3rd ed. Oxford University Press, New York, 348 p.

Nikitin, W. (1936) *Die Fedorow-Methode*. Verlag Gebrüder Borntraeger, Berlin, 109 p.

Phillips, W.R. (1971) *Mineral Optics: Principles and Techniques*. W.H. Freeman and Company, San Francisco, 249 p.

Reinhard, M. (1931) *Universal Drehtischmethoden. Einführung in die kristalloptischen Grundbegriffe und die Plagioklasbestimmung*. B. Wepf & Cie, Basel, 119 p.

Slemmons, D.B. (1970) *Universal Stage Procedures*. Department of Geology, MacKay School of Mines, University of Nevada, Reno, 14 p.

Stöffler, D., and Langenhorst, F. (1994) Shock metamorphism of quartz in nature and experiment: I. Basic observation and theory. *Meteoritics*, **29**, 155-181.

Su, S.-C., Bloss, F.D., Ribbe, P.H. (1984) Optic axial angle, a precise measure of Al,Si ordering in T1 tetrahedral sites of K-rich alkali feldspars. *American Mineralogist*, **69**, 440-448.

Tröger, W.E., Bambauer, H. U., Taborsky, F., and Trochim, H.D. (1979) *Optical Determination of Rock-Forming Minerals* [English edition]. E. Schweizerbart'sche Verlagsbuchhandlung, Stuttgart, 188 p.

Wilcox, R.E. (1959) Universal stage accessory for direct determination of the three principal indices of refraction. *The American Mineralogist*, **44**, 1064-1067.

Winchell, A.N., and Winchell, H. (1951) *Elements of Optical Mineralogy, Part II: Descriptions of Minerals*, 4th ed. John Wiley and Sons, Inc., New York, 551 p.

Wright, F.E. (1911) *The Methods of Petrographic-Microscopic Research: Their Relative Accuracy and Range of Application*. Carnegie Institution of Washington, Publication no.158, 204 p.

Acknowledgements

The author wishes to thank John Delly, College of Microscopy, Westmont, Illinois; Mickey Gunter, University of Idaho; and Olaf Medenbach, Ruhr University, Germany, for their thoughtful reviews of this paper.

Any use of trade, firm, or product names is for instructive purposes only and does not imply endorsement by the U.S. Government.

Using the Universal Stage to decode the cryptic cooling record of igneous rocks

Marian B. Holness
Department of Earth Sciences, University of Cambridge, Downing Street, Cambridge CB2 3EQ, UK.

Decoding rock history is very much detective work: we can use the mineral assemblage, the structure of individual minerals, or the way in which its constituent mineral grains fit together to create a picture of how it got to where it is now. Having been exposed at an impressionable age to the Natural Sciences course at Cambridge University, where I studied materials science, metallurgy and physics before specialising in geology, it's the third approach that interests me most. This catholic education opened my eyes to textural features that might otherwise have passed unnoticed, and using Cambridge's vast collection of metamorphic and igneous thin sections (165,000 and still counting) gave me a lasting feeling that the way into most geological problems lies down the microscope. I count myself lucky to have been taught optical mineralogy as an undergraduate, to be teaching these courses myself to the current generation of undergraduates, and to be in a department with a long tradition of petrography: I work in the shadow of greats such as Alfred Harker (who started the enormous collection which bears his name), Cecil. E. Tilley, Alec Deer and Stuart Agrell.

My current efforts are centred on the problem of solidification. When chemically complex liquids such as magmas solidify, they generally begin by crystallising a single phase. As this phase is progressively removed from the liquid the composition of the remaining liquid changes until it become saturated in another phase that begins to crystallise along with the first. The process continues, with progressive arrivals on the liquidus (or disappearances due to peritectic reactions) until solidification is complete. The complexity of the problem arises from the possibility of relative movement of solid and liquid. Gravitational settling of solid phases to the floor of the magma reservoir, or concentration of nucleation and growth on the margins of the reservoir, creates a mushy layer. If residual liquid can be extracted from this mushy layer, either by diffusion or by gravitationally-driven compaction, this will drive the composition of the liquid remaining in the bulk reservoir towards progressively more evolved compositions. Upwards-flow of expelled liquid may also create opportunities for reaction and metasomatism as these evolved interstitial liquids encounter higher levels of the mush. The behaviour of the mushy layer therefore has enormous influence on the evolution of magmas (and hence their eruptive style), the concentration of economic deposits of ore minerals, and the timing of eruptions. Understanding this intriguing problem involves constraining the physical properties of the mush: we need to know about its mechanical response to compaction, disruption and slumping, as well as to document the progressive occlusion of porosity and destruction of permeability. My first steps in the attempt to find a solution are directed at using grain boundaries to track the cooling history of solidifying plutons.

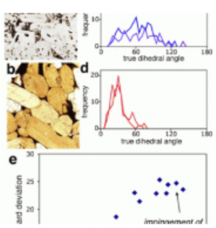

Figure 1

In the earliest stages of solidification, crystals essentially grow unimpeded: they generally adopt shapes controlled by the relative rates of growth of different faces, forming typical euhedral forms such as the tabular habit of plagioclase or elongate amphibole prisms. As solidification proceeds, these individual crystals begin to impinge on each other. If growth is sufficiently rapid, the crystals continue to grow with planar faces, dictated by the drive towards chemical equilibrium. This creates a mush with a pore structure first described by Elliott et al. (1997) as an impingement texture (Figure 1a). The angles formed by the impingement of these planar faces, forming the corner of a melt-filled pore, vary widely and depend on the random juxtaposition of adjacent grains. However, the median value of a population of these angles will be 60°, since the sum of included angles in a triangle is 180°. If the system is held at a constant temperature, or is allowed to cool extremely slowly, it will attempt to further reduce its total internal energy by minimising the amount of energy tied up in grain boundaries and interfaces. This process of textural equilibration involves the migration of interfaces towards the position of lowest energy. Typical of an equilibrated texture is the development of characteristic angles at the pore corners due to the balancing of interfacial energies at these junctions, together with the creation of interfaces with constant mean curvature (Figure 1b). This angle, known as the dihedral angle, is generally in the range 20 - 40° for a silicate liquid-solid aggregate and is very important in controlling pore structure and permeability. A monomineralic system with negligible anisotropy of interfacial energies (i.e. a single value of dihedral angle) contains an interconnected series of channels on three-grain edges even down to vanishingly low porosities if the melt-solid-solid dihedral angle is less than 60°: this is the case for all partially molten silicate systems of geological importance (e.g. Holness, 1996). Importantly, however, no mineral is completely isotropic with respect to interfacial energies: there will be a range of dihedral angles in a texturally equilibrated mush (Figure 1d) so some three-grain edges will be dry while others contain a fluid-filled channel (Laporte & Provost, 2000). We need to know what this range is, and this is where the Universal Stage comes into its own.

Measuring the characteristics of a population of angles between grain boundaries is something that has been done by the metallurgical community for some time. Since they are dealing with optically opaque materials they developed ways of interpreting the population of angles measured on a polished section, i.e. a random cut through a 3-D material. Early work by geologists followed suit, with many published studies documenting the variations of the median of a population of angles in geological systems, all measured on a conventional microscope stage. The median of such a population is very close to the true median of the population (Riegger & Van Vlack, 1960) but we lose valuable information by confining ourselves to this simple measure: what we really need is an idea of the true range of angles. While it is possible to construct numerical models which can be used to predict what a complex population might look like in a random 2-D cut, there is nothing like direct observation to constrain it properly and, of course, direct observation doesn't rely on model-dependent assumptions. As pointed out by Ron Vernon (1997) this can be neatly and elegantly achieved for rocks if you use a Universal Stage: any three-grain junction can be rotated so that the true angle between grain boundaries can be measured, and the true spread of the population can be observed. There is currently no other way of doing this - the Universal Stage is the only instrument capable of collecting this information. The Universal Stage also has the great advantage of letting us measure all angles in a section, even those cut so obliquely that they can't be properly seen on a conventional stage - this is particularly important in a coarse-grained sample in which the number of suitable junctions may be small.

There is more useful information encoded in the angles at pore corners in melt-bearing rocks. The median and standard deviation provides a measure of how close the crystal mush has approached textural equilibrium. A mush which is actively solidifying (e.g. Figure 1a) will have a population of

GN140 Content

angles with a median of 60° and a high standard deviation (Figure 1c), while one which is experiencing a period of constant temperature, and has therefore stopped crystallising, has the opportunity to reach textural equilibrium (Figure 1b): this will result in an angle population with a lower median and a lower standard deviation (Figure 1d). A suite of glass-bearing amphibole-dominated crystal nodules erupted by recent alkali basalt eruptions in Western Turkey shows this process frozen in time (Figure 1e). While some of the nodules have dihedral angle populations indicative of continuing crystallisation interrupted only by entrainment and eruption, other nodules provide evidence that they remained at high constant temperatures for a while, permitting variable extents of approach to textural equilibrium at the pore corners (Holness et al., 2005).

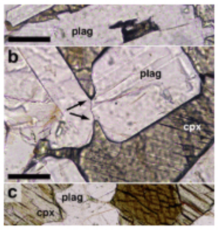

Figure 2

If we now consider a continuously crystallising system we need to think about the nucleation and growth of a second solid phase in the melt-filled pores. These pore-filling, or interstitial, phases commonly inherit the shape of the melt-filled pore, including the angles at the pore corners (Figure 2a). Irrespective of whether these pores had reached textural equilibrium or whether they still had the growth-controlled impingement texture, the median angle of the population inherited by the interstitial solid is much lower than that expected for solid-solid textural equilibrium (Figure 2c). These solid-state angles are of the order of 120°, since grain boundary energies are very similar regardless of the solid phases involved (Vernon, 1968). If the now-solid igneous rock is cooled slowly enough, it will attempt to reduce its internal energy by rotating grain boundaries into these higher angles (Figure 2b), and the extent to which it can do this is a function of its time-integrated thermal history (Holness et al., 2005). The angle population therefore provides an easily accessible measure of how long the rocks stayed hot. Since the closure temperature for this solid-solid dihedral angle change is rather high (it is accomplished by significant diffusive mass transport via grain boundaries) we can use the angle population as a thermal probe for processes occurring close to the magma-mush interface.

This provides us with an astonishingly sensitive new tool: a nice example of serendipity in science. One of the most powerful ways of using dihedral angles is to track changes in the liquidus assemblage. When I first started this work I concentrated on the plagioclase-rich cumulates of the Rum Layered Intrusion in which augite fills in gaps between the earlier-crystallising plagioclase grains. I discovered that the pyroxene-plagioclase-plagioclase angles in all the gabbroic layers (in which plagioclase, augite and olivine are liquidus phases) had medians hovering around 90°, while those in the troctolitic layers (in which only plagioclase and olivine are on the liquidus) were in the region of 80°. I had absolutely no idea why this might be until I looked at the Layered Series of the Skaergaard. Unlike Rum, which was an open chamber with a consequent random jumble of cumulate layers, Skaergaard crystallised as a closed system, with the liquid tracking down the phase diagram. The Layered Series is thus a set of progressively more fractionated layers and it was immediately apparent that the arrival of cumulus augite near the base of the chamber made the median pyroxene-plagioclase-plagioclase angle jump from about 80° to 100° (Holness et al., 2007a, b). The reason for this is absolutely fundamental and is to do with the change in slope of the liquidus at the arrival of a new phase. This change in slope means there is a step-change in the fractional contribution of the latent heat of crystallisation to the total enthalpy budget, and so the pluton takes longer to cool down: the cumulate have more time to approach textural equilibrium.
Materials scientists have known about this effect for a long time - many undergraduate courses include an experiment tracking the temperature of a crystallising binary system in a beaker on the benchtop - but this is the first time we have found a way of decoding fully crystalline rocks to detect the same thing. Suddenly there are a whole lot of interesting questions we can ask: at the moment I am busy using this new information to constrain the thickness of the mushy layer within the Skaergaard intrusion. It looks as though there was an unstable highly porous mushy layer on the walls, which got progressively thicker with time, reaching a maximum of about 200m. The continual erosion of the wall mush created detrital fans on the floor where the mush may have been several hundreds of metres thick: but far from the walls the floor mush was a few metres thick - crystallisation essentially occurred at a hardground.

Although it is possible to get an approximate idea of textural change using a conventional stage, the Universal Stage makes it possible to extract extraordinarily detailed information about cooling histories. Measuring angles is not difficult - it certainly doesn't exploit the full potential of the U-stage and the technique is very easy to learn - and perhaps the biggest obstacle is actually getting your hands on a functioning U-stage. I have derived immense satisfaction over the last few years in giving these beautiful and sophisticated instruments another lease of life, obtaining hitherto inaccessible information on the cooling history of igneous rocks.

References
Elliott, M.T., Cheadle, M.J. & Jerram, D.A. (1997) On the identification of textural equilibrium in rocks using dihedral angle measurements. Geology, 25, 355-358.

Holness, M.B. (2006) Melt-solid dihedral angles of common minerals in natural rocks. Journal of Petrology, 47, 791-800.

Holness, M.B, Cheadle, M.J., & McKenzie, D. (2005) On the use of changes in dihedral angle to decode late-stage textural evolution in cumulates. Journal of Petrology, 46, 1565-1583.

Holness, M.B., Nielsen, T.F.D. and Tegner, C. (2007a) Textural maturity of cumulates: a record of chamber filling, liquidus assemblage, cooling rate and large-scale convection in mafic layered intrusions. Journal of Petrology, 48, 141-157.

Holness, M.B., Tegner, C., Nielsen, T.F.D., Stripp, G., and Morse, S.A. (2007b) A textural record of solidification and cooling in the Skaergaard Intrusion, East Greenland. Journal of Petrology, 48, 2359-2377.

Laporte D., & Provost, A. (2000) Equilibrium geometry of a fluid phase in a polycrystalline aggregate with anisotropic surface energies: Dry grain boundaries. Journal of Geophysical Research, 105, 25937-25953.

Riegger, O.K. & Van Vlack, L.H.W. (1960) Dihedral angle measurement. Transactions of the Metallurgical Society of the AIME, 218, 933-935.

Vernon, R.H. (1997) Comment: On the identification of textural disequilibrium in rocks using dihedral angle measurements. By Elliott, M.T. & Cheadle, M.J. Geology, 25, 1055.

Vernon, R.H. (1968) Microstructures of high-grade metamorphic rocks at Broken Hill, Australia. Journal of Petrology, 9, 1-22.

Arctic Russia: Minerals and Mineral Resources

G.P. Glasby and Yu.L. Voytekhovsky
Geological Institute, Kola Science Centre, Russian Academy of Sciences, Fersman Str. 14, Apatity 184209, Murmansk Region, Russia

'Arctic must be conquered and it is especially important for direct industrial development of mankind, at least the same as the triumph of knowledge. The victory may be deemed complete, however, only if a vessel outfit in Europe goes fast and directly to the Bering Strait... Russia is to crave for true victory over Arctic Ocean even more than any other country, for none else owns greater length of shore line in the Arctic Ocean...'
-'Arctic Ocean investigation' by Dmitri Mendeleyev, 1901

'The basic economic law of socialism - the law of the continuous growth and improvement of socialist production on the basis of superior techniques for the purpose of cultural requirements of the whole of society - determines the need to draw ever new raw material and power resources to economic use.'
-S.V. Slavin 1972, Head of the Economic Research Bureau, Glavsevmorput 1972, 1982 (Luzin et al. 1994, p. 6)

Introduction

Figure 1

The Arctic Circle is usually defined as being at 66° 33' 39" north of the Equator. For comparison, the latitude of Moscow is 55° 33'N. In this case, the area of the Russian Arctic is quite broad extending up to 10° of latitude. However, an alternative definition of the Arctic region is that area where the average temperature in the warmest month lies below 10°C. This is marked on the accompanying map in red (Fig. 1). Based on this definition, it is seen that the northern boundary of the Arctic varies by more than 6° of latitude and occupies a relatively thin sliver of northern Russia.

Figure 2

To the north of the Russian Mainland lie a number of major islands. These include Franz Josef Land which consists of 191 ice-covered islands and is the most northerly territory of Russia, Novaya Zemlya (New Land) which separates the Barents Sea from the Kara Sea, Severnaya Zemlya (North Land) which separates the Kara Sea from the Laptev Sea and the New Siberian islands. Fig. 2 gives an impression of the Arctic North as seen by satellite. AMAP (1998) gives an excellent account of the physical and geographical characteristics of the Arctic region with many outstanding figures. Interestingly, the Kola region is three to four times the size of countries such countries as Belgium, the Netherlands, and Denmark.

Murmansk is Russia's only ice-free port in the Russian Arctic. It opened in 1915-16 when the railway line from Leningrad (now St. Petersburg) to Murmansk was built. In 1925, A.E. Fersman discovered huge deposits of apatite (1Gt) and urtite (10Gt) in the Khibiny Mountains which were eventually exploited in the mid-1930s (Glasby 2008). Murmansk suffered massive destruction (second only to Stalingrad) when the Germans launched an offensive in 1941 but fierce Soviet resistance prevented the Germans from capturing the city.

The main economic interest in the northern part of Russia is, of course, its natural resources including oil and gas. The average population density of Russia is very low. In parts of Russia, you could go for months without meeting anybody.

Development of the Russian Arctic

The development of icebreakers was crucial to the opening up of the Russian Arctic. This required advances in shipbuilding technology to create the icebreaker, a vessel strong enough to withstand the crushing power of the ice and to break through it. In 1916, the first icebreaker aimed at supporting regular navigation along the northern coast of Russia was built in Newcastle by order of the Russian Maritime Ministry and named Krasin. The icebreaker operated for many years in the Arctic and was crucial to the development of the Northeast Passage. In 1928, Krasin reached the ice camp of the Italian airman Nobile and took part in his rescue.

Figure 3

The first nuclear powered icebreaker, *Lenin*, was built in 1959 at the Admiralty shipyard in Leningrad (now St. Petersburg) which I passed every day when I worked there! The most powerful nuclear icebreaker in the world was *Soviet Arktika* which was built in 1975 and shut down in 2008. It was the first surface ship to reach the North Pole in 1977. Icebreakers were therefore the platform for opening up Arctic Russia. Figs 3 and 4 show the nuclear-powered icebreakers, 'Taimyr' and 'Vaigach', in action.

On August 2, 2007, Russia used two Mir submersibles to perform the first manned descent to the seabed under the geographical North Pole to a depth of 4,261 m in order to study the region in relation to Russia's territorial claim to the region extending from Russia to the North Pole made in 2001. The pilot of Mir 1 was Anatoly Sagelevich, Russia's most experienced submersible pilot. At the seafloor, the Mir crew planted a one metre tall Russian flag made of titanium alloy and collected sediment samples. The descent was supported by the nuclear powered icebreaker *Rossiya* with the power to negotiate the most challenging ice in the Arctic Ocean (Birch 2007). When the submersibles ascended, the pilots had to locate the hole through which they had descended which had already drifted one mile. Anatoly Sagelevich was awarded the title of Hero of the Russian Federation for 'courage and heroism shown in extreme conditions and successful completion of the High-latitude Arctic Deep-Water Expedition.' In the west, several commentators

GN140 Content

Figure 4

described the dives as a stunt but, in this, they were underestimating a formidable achievement. Fig. 5 shows the launching of the 'Mir-1' during a routine scientific survey.

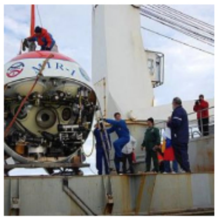

Figure 5

Figure 6

The rationale for this expedition was, of course oil (Shoumatoff 2008). According to some estimates, 25% of the world's remaining fossil fuel reserves are located in the Arctic Ocean. With the Arctic ice cap shrinking by 28,000 sq. miles (70,000 km^2) per year, gigantic pools of open water are appearing in the ice, the possibility of commercial recovery of this oil are increasing year by year. In fact, the Russians are claiming the right to the oil, gas and minerals of the Arctic Ocean up to the North Pole based on the extension of the Lomonosov Ridge which runs 1,210 miles from Siberia through the North Pole almost to the junction of Ellesmere Island and Greenland. The dive was designed to bolster Russia's claim to about 460,000 sq miles (1.15×10^6 km^2) of territory on the Lomonosov and Mendeleyev Ridges which the Russians claim are part of the Russian continental shelf. U.S. Geological data suggests that the Arctic Seabed contains up to 25% of the world's oil and natural gas reserves and other mineral resources which are being made accessible by the receding polar ice caused by global warming. Fig. 6 shows the icebreaker *Vaigish* arriving in Dixon which is located on the Taymyr Peninsula between the Kara Sea and Laptev Seas and Fig. 7 the Laptev Sea which was discovered by Khariton and Dmitri Laptev in 1739-1742.

Mineral Deposits

Figure 7

Arctic Russia has a huge potential for the production of minerals. For example, 91% of natural gas production and 80% of Russia's explored reserves of explored natural gas are located in the Arctic. The Arctic also contains 90% of its offshore reserves of hydrocarbons. According to Burakova (2005), the estimated value of Arctic minerals was $1.5-2 trillion. In addition, there were 25 mines operating in Arctic Russia in 2006 (Anon 2006a). The majority of these mines were Ni-Cu mines but Sn, U and phosphate were also mined. Because the last ice age removed the topmost sediment layer of the soil, the Kola Peninsula (which occupies an are of 129,500 km^2) is extremely rich in various ores and minerals, including apatite, alumina, iron ore, mica, titanium, phlogopite and vermiculite. The Kola Superdeep borehole is also located on the Kola Peninsula near the Norwegian border. The deepest hole was SG-3 which reached a depth of 12,261m in 1989 drilling rocks 2.7 G yrs old and releasing large quantities of hydrogen gas (Fuchs et al. 1990). Fig. 7 shows the Laptev Sea which is located between the Kara Sea and East Siberian Sea and between the Taymyr Peninsula and Severnaya Zemlya in the west and the New Siberian Islands in the east. It has an area of 250,900 sq mi (649,800 km^2) and is relatively shallow. The sea remains frozen throughout the year, except for the months of August and September. The Lena River is the major tributary draining into the sea. The sea is named after Khariton and Dmitri Laptev, two Russian cousins who were a part of the second Arctic expedition led by Danish mariner Vitus Bering in 1739-1742.

The subsurface of the Kola Peninsula contains a remarkable abundance of various minerals. Among the elements of interest are copper, iron, nickel, cobalt, titanium, rare metals, ceramic raw materials, mica and precious stones. An excellent account of the geography and climate of the Murmansk region is given in http://www.b-port.com/en/info/region/

A large part of the almost 20 Mt of ore mined annually in Russia consists of apatite and nepheline. Three-quarters of the phosphate fertilizer in Russia is manufactured from apatite concentrate from the Khibiny deposit located on the Kola Peninsula. Nepheline is used in the manufacture of soda and potash for the chemical industry. Enormous quantities of soda are required to produce alumina from bauxite and in making glass.

The Kola Peninsula also contains large reserves of precious stones, the most important of which are amazonite and amethyst. Hundreds of millions of years ago, crusts, known as 'druses', meaning crusts of projecting crystals lining rock cavities, of variously colored quartz, fluorite, barite, calcite and other minerals formed on the walls of tectonic cracks surrounding the Kola Peninsula. The most interesting of these are the quartz crystal druses, smoky quartz, black quartz and especially amethyst which is noted for its wide range of colors from soft lilac to rich dark violet. Amethyst is classified as a gem-quality mineral and is often found in nature in the form of separate, sometimes large-sized crystals. Amethyst in the form of crystalline bunches is extremely rare in nature but the largest and best known deposits of this type are located on the Kola Peninsula.

It has been estimated that the recoverable reserves of the oil and gas fields of the Russian continental shelf amount to 100 billion tonnes of which oil and gas make up 13 and 87%, respectively (Anon 2006b). Of these fields, 44.4% are located in the Kara Sea, 25.6% in the Barents Sea, 8.8% in the Okhotsk Sea and 5.1% in the Pechora Sea. In the Okhotsk Sea, 3.5 10^9 m^3 of gas hydrates were identified within an area of about 4.36 km^2. Overall, it has been estimated that there are between 2.10^{14} and $7.6.10^{18}$ m^3 of gas hydrates located on the world's continental shelves making these deposits a huge potential resource (Anon 2006b). However, the bulk of the gas hydrates exist close to their stability boundary and minor changes in temperatures and pressure could lead to huge emissions of gas. Nonetheless, both Japan and the USA plan to start commercial production of the gas hydrates between 2010 and 2015. There are also abundant placer deposits on the continental shelves of which gold and tin are economically the most important. Placer diamonds, amber and fossil ivory are also present. Of the bedrock deposits, a few tens of millions of tonnes of Pb-Zn carbonate deposits have been located on the Novaya Zemlya Archipelago. Manganese is mainly associated with carbonate ores in Permian deposits in Novaya Zemlya which are estimated to contain 3 billion t of ore to a depth of 500 m.

Of particular interest are the huge deposits of Ni which were discovered at Pechenga in what was then Finland (northern part of the Kola Peninsula) in the 1930s. The principal minerals of economic interest were pentlandite, pyrrhotite and chalcopyrite. The Pechenga district includes numerous massive and disseminated Ni-Cu sulphide ore deposits associated with mafic-ultramafic igneous rocks. In 2002, reserves of the deposit were estimated to be 30 Mt at 2% Ni, 1% Cu and 0.4% Co but the deposits also contain significant concentrations of arsenic (Abzalov et al. 1997) and the Platinum Group Elements (Distler et al. 1990). After the war, Norilsk Nickel plant became the largest mine in the Russian Arctic where it was best known for its high levels of pollution, mainly of SO_2, which caused major health and environmental problems and created a barren area for kilometres around. In 2006 and 2007, Norilsk's operations in Russia featured as among the 'world's top ten polluted places'. The impact of this pollution from smelters in the Kola Peninsula has been documented in considerable detail by Dauval'ter et al. (2009). As an example, it was estimated that 310 t of Ni, 120 t of Cu, 14 t of Co, 19 t of Zn, 0.087 t of Cd, 0.78 t of Pb and 0.053 t of Hg were deposited in Lake Kuetsjarvi over a 60 year period as a direct result of the mining and refining activities in the area (Dauvalter 2003). Dauval'ter and Il'yashhuk (2007) have also described the conditions for the formation of ferromanganese concretions in the lakes of the

Kola Peninsula.

The Norilsk plant was closed down in 2008 because the extreme levels of pollution. In July, 2007, the last measurement of SO2 concentrations at the monitoring stations showed a median value of 7500 milligram sulphur per m3 for one hour. This was more than 20 times more the maximum recommended level of 350 milligram per m3. Later on, the Norilsk Nickel plant amalgamated with the Severonickel and Pechenganickel plants in the Kola Peninsula. Although the conditions encountered at the Norilsk Nickel plant were extreme, they are typical of many of the smelters in Russia which are surrounded by barren areas stretching for miles. As a result of SO2 emissions from smelters, Arctic haze is a common phenomenon in northern Russia (Arnold et al 2009).

Norilsk Nickel is now one of the biggest mining groups in the world. In 2007, it produced 18.8% of the world's Ni, 46.3% of the world's Pd and 12% of the world's Pt.

For those with an historical bent, the review by Luzin et al. (1994) gives an outstanding account of the socialist development policy of resources (including mineral resources) in the Kola Peninsula and elsewhere which prevailed during communist times. This policy favoured intensive resource extraction and industrialization above all and resulted in increased settlement in the northern part of the peninsula, much of it involuntary. It led to the opening of new mines and the construction of smelters and refining facilities which resulted in severe environmental damage in the region and beyond because of the lack of environmental controls. This legacy is still clearly apparent in the Kola Peninsula and elsewhere today.

Environmental Pollution

Because of its remoteness and huge size, it might be expected that the Russian Arctic would be a pristine environment with minimal pollution. However, there are several major types of environmental impacts in the Russian Arctic as a result of waste discharges during offshore oil and gas activity (Patin 1999), smelting of ore deposits to produce metals (Norseth 1994; Dauval'ter et al. 2008) and nuclear weapons testing. Pollution is a serious problem wherever smelting is taking place. In such areas, the landscape is often degraded to a barren wilderness as far as the eye can see.

The Kola Peninsula as a whole suffered major ecological damage, mostly as a result of pollution from military (particularly naval) production, as well as from the mining of apatite. About 250 nuclear reactors produced by the Soviet military remain on the peninsula. Though no longer in use, they still generate radiation and leak radioactive waste.

Regretably, these environmental problems have a global dimension which we have not yet managed to solve (Glasby 1991).

Global warming

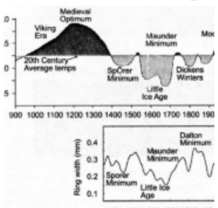

Figure 8

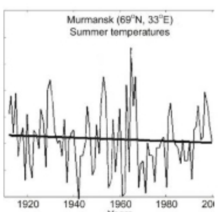

Figure 9

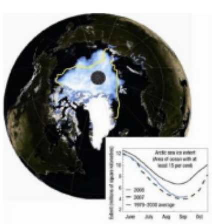

Figure 10

It is widely accepted that global warming is taking place. To evaluate the validity of this process in the Russian Arctic, a detailed study of tree rings in juniper trees from at 69° N, 33° E in the northern Kola Peninsula was undertaken in 2004 (Shumilov et al. 2007). From this, it was possible to build up a 676 year long chronology and use this to establish patterns of climate variation over this period. The tree ring data identified minima of solar activity at 1416-1534 (Spoerer Minimum), 1645-1715 (Maunder Minimum) and 1801-1816 AD (Dickens winters) and showed a close relationship to known global palaeo temperatures in Europe (Fig. 8).

Records were also taken of summer temperatures at this location between 1920 and 2000 and showed a steady decrease in temperature of about 0.2° C over this period (Fig. 9). According to Shumilov and his colleagues, past climate changes in the Kola Peninsula are best related to changes in solar and galactic cosmic ray activity rather than increases in the concentration of atmospheric CO2 as is commonly assumed. As result of global warming, the freeze up period for the Northern Sea route will shorten significantly over the next 15 years (Burakova 2005).

Daly (2003) has also made a convincing case that global warming is a function of the temperature of the sun and is unrelated to the concentration of greenhouse gases in the atmosphere (http://www.john-daly.com/solar.htm)
In the oceans, the seasonal minimum for Arctic ice in 2008 was recorded on 14 September at 4.52 x 10^6 m^3. This was the second lowest value ever recorded and it was estimated that, at the present rate of melting, the Arctic would have no sea ice left by 2060 (Serreze and Stroeve 2008) (Fig. 10).

Arctic Haze

One of the hazards of the Arctic is Arctic haze which is the visible reddish brown haze which occurs at high latitudes. It was first noted in the 1950s by Canadian pilots puzzled by low visibility over pristine ice. The haze contains gaseous species such as SO_2 and NOx as well as aerosols containing SO_4^{2-}, H^+, NH_4^{2+} and metals.

The haze is seasonal and peaks in spring. It is most severe when stable high pressure systems produce calm, clear weather at mid-latitudes. It was long thought to be caused by burning coal at mid latitudes. However, recently collected evidence suggests that Arctic haze may, in fact, be caused by forest fires and agricultural burning in Asia (Brock et al 2009). This would explain the increase in atmospheric haze over the last decade despite lower emissions from Russian factories.

In April 2008, NOAA aircraft made six sorties from Alaska to the Arctic Ocean in order to sample this haze (Perkins 2009). They identified nearly 50 separate plumes of haze occurring at altitudes up to 6.5 km above the ocean. The plumes were made up of tiny black particles of carbon averaging 300 nm in diameter. Analyses indicated that the plumes contained little propane or tetrachloroethene which would indicate an industrial origin supporting the idea that these plumes are the result of forest fires. Pollution from growing economies such as China may also be adding to the haze. This pollution is resulting in the Arctic warming faster than any other area of the globe.

Smelters

Smelting in Russia is a highly polluting operation which disfigures the local environment (Kozlov 1995).

One of the largest enterprises in N.W. Russia is the Kola mountain - metallurgical company which was created in 1998 as a result of the amalgamation of Norilsk Nickel located in western Siberia with Severonickel and Pechenganickel from the Kola Peninsula which had already been in operation for over 40 years to form a single complex.

Figure 11

Figure 12

Severonickel is located at Monchegorsk (Fig. 11). It produced black nickel for the first time in February, 1939, and one year later clean nickel. In 1982, there was a substantial expansion of the operation for processing ore material from Norilsk that enabled 'Severo nickel' to become the largest manufacturer of clean nickel in the world. In January, 2003, a new plant for the production of copper with an annual capacity of 15,000 t was brought into operation using modern technology which enabled considerable savings in industrial expenses to be made and a substantial reduction of the amount of industrial gases released to the atmosphere. However, Monchegorsk is still the scene of massive environmental degradation. Elana Wilson, a visiting American student, has presented a moving account of the environmental destruction of Monchegorsk (Wilson 2000). Monchegorsk was a planned city on the shores of Lake Imandra designed by architects from St. Petersburg in the 1930's with wide boulevards and colourful buildings and intended to reflect proletarian ideals of the still-young Soviet Union by striking a balance between industry, culture and aesthetics in both its design and societal structure. Now Monchegorsk and the surrounding area is classified as a 'Zone 1' area of pollution, and defined as technogenic barren (Figs 12-14). In such cases, there is complete destruction of tundra and boreal forest vegetation. In all, more than 8000 km^2 of larch forest and lichen, essential sustenance for the reindeer herds maintained by Nenets and Sámi, have been wiped out by acid rain since 1980 alone and hundreds of km^2 of tundra have been rendered sterile.

Figure 13 and 14

Pechenganickel is located in Zepoliarniy near the town of Polar in the north-west part of the Kola Peninsula. The enterprise started in 1946 and processed ore located near small mines. Now the plant mines nickel and copper sulphide ore with 0.6-1.7% Ni and 0.3-0.77% Cu and enriches it with ore from the main Norilsk plant for metallurgical processing. Its main products are matte and sulphuric acid.

Although the situation is improving, mining in Russia has generally been carried out with little regard for the environment.

In both 2006 and 2007, Norilk's operations in Russia featured amongst the world's top ten most polluted places.

Nuclear weapons testing

The Soviet Union also carried out extensive testing of nuclear weapons on the Novaya Zemlya archipelago in the Barents Sea. In all, 130 tests were carried out in the period 1955 to 1990 at three main locations at latitudes between 71°N and 74°N (Khalturin et al. 2005). These tests involved 224 separate explosive devices, including by far the largest atmospheric and underground tests in the Soviet Union. In all, about 265 megatons of nuclear explosive energy were released during these tests. In these test programmes, the Soviet Union was mainly catching up with the United States which had a lead of about 4 years in its testing programme. In 1961, the Soviet Union exploded its most powerful atmospheric bomb which weighed 26 tonnes and was too large to be placed in the aircraft and had to be fastened underneath. The most powerful underground nuclear tests (UNTs) took place in September and October 1973. The seismic magnitude of these two tests was 6.97 and 6.98 and the total yield was 4.2 mt. These two tests produced very different results. In one case, four small ridges were created and a region 120 m in width was uplifted 2 to 3 m. In the other, a huge landslide occurred and 80 million m^3 of material cascaded down in a massive rock avalanche and formed a 2 km long lake behind the debris. About 250 nuclear reactors belonging to the Soviet military remain on the Kola Peninsula. Although no longer in commission, they still generate radiation and leak radioactive waste.

Conclusions

Arctic Russia plays a key role in the Russian economy. It is particularly noted for its mineral wealth but also plays a key role in shipping. There is no doubt that the Russian Arctic will play an increasing role in the Russian economy as a result of global warming which will facilitate shipping and mining there. However, the region has been subjected to gross environmental stress, particularly during Soviet times, which still play a significant role even now. The main aim for the future should be the development of a new environmental policy in Russia which will put responsible environmental stewardship as a major goal for the future. At present, Russia's environmental standards fall well below those of the European Union.

References

Anon 2006a. To the ends of the earth. Mining Magazine 194 (2), 22-25.

Anon 2006b Mineral Resources of the Russian Shelf Special Issue.115 pp.

Abzalov, M.Z., Brewer, T.S., Polezhaeva, L.I. 1997. Chemistry and distribution of accessory Ni, Co, Fe arsenic minerals in the Pechanga Ni-Cu deposits, Kola Peninsula, Russia. Mineral. Petrol. 61, 145-161.

AMAP 1998. AMAP Assessment Report: Arctic Pollution Issues Chapter 2: Physical/Geographical Characteristics of the Arctic, pp. 9-24.

Arnold, F. et al. 2009. Central Arctic Atmospheric SO_2 pollution from smelters: Airborne detection and Arctic Haze formation. Geophysical Research Abstracts, Vol. 11, EGU2009-3560-1.

Birch, D. 2007. Russian Arctic team reaches North Pole. The Washington Post August 1.

Brock et al. 2009. Biomass burning in Siberia and Kazakhstan as an important ... Geophysical Research Letters 36: L022813-1.

Burakova, I. 2005 Development of Arctic areas to bring trillions dollars of profit to Russia. Pravda (21.04.05)

Daly, J.L 2003. Days of sunshine (http://www.john-daly.com/solar.htm)

Dauval'ter, V. 2003. Impact of mining and refining on the distribution and accumulation of nickel and other heavy metals in sediments of subarctic Lake Kuetsjarvi, Murmansk Region, Russia. J. Environ. Monitoring 5: 210-215.

Dauval'ter, V.A., Dauval'ter, M.V., Saltan, N.V., Semenov, E.N. 2009. The chemical composition of surface water in the influence zone of the Severonickel smelter. Geochem. Internat. 47 (6): 592-610.

Dauval'ter, V.A., Il'yashuk, B.P. 2007. Conditions of formation of ferromanganese nodules in the bottom sediments of lakes of the Baltic Shield. Geochem. Int. (45 (6): 624-631.

Distler, V., Fillmonova, A., Grokhovskaya, T., Laputina, I. 1990. Platinum-Group Elements in the copper-nickel ores of the Pechenga ore field. Int. Geol. Revs 32: 70-83.

Fuchs, K., Kozlovsky, E.A., Krivtsov, A.I., and Zoback, M.D. (eds.) 1990. Super-Deep Continental Drilling and Deep Geophysical Sounding. Springer Verlag, Berlin, 436 pp.

Glasby, G.P. 1991. A review of the concept of sustainable management as applied to New Zealand. Jl R. Soc. N.Z. 21: 61-81.

Glasby, G.P. 2007. A.E Fersman and the Kola Peninsula. Geoscientist 18 (7): 20-25.

Khalturin, V.I., Rautian, T., Richards, P.G., Leith, W.S. 2005. A review of nuclear testing by the Soviet Union at Novaya Zemlya, 1955-1990. Science and Global Security 13: 1-42.

Kozlov, M.V, Haukioja, E., Bakhtiarov, A.V. and Stroganov, D.N. 1995. Heavy metals in birch leaves around a nickel-copper smelter at Monchegorsk, northwestern Russia. Environmental Pollution 90: 291-299.

Luzin, G.P., Pretes, M. and Vasiliev, V.V. 1994. The Kola Peninsula: Geography, History and Resources. Arctic 47: 1-15.

Moiseenko, T. 1995. Critical loads of SO_4 for surface waters in the Kola region of Russia. Water, Air, and Soil Pollution 85: 469-473.

Norseth, T. 1994. Environmental pollution around nickel smelters in the Kola Peninsula Russia. Science of the Total Environment 148: 103-108.

Patin, S. 1999. Environmental impact of offsore oil and gas industry. Ecomonitor Publ. 448 pp.

Perkins, S. 2009. Plumes of Arctic haze traced to Russia, Kazakhstan. Science News 175(6), p.13.

Serreze, M.C. and Stroeve, J.C. 2008. Standing on the brink. Nature Reports Climate change. Published online: 9 October 2008 Corrected online: 13 October 2008 (doi:10.1038/climate.2008.108)

Shoumatoff, A. 2008. The Arctic oil rush. Vanity Fair May

Shumilov, O.I., Kasatkina, E.A., Lukona, N.V., Kirtsideli, Yu and Kanatjev, A.G. 2007. Paleoclimatic potential of the northernmost part juniper trees in Europe. Dendrochronologia 24, 123-130.

Wilson, E.A. 2000. Monchegorsk: City of Ideals and Difficult Realities. Available on the internet.

Report on Minerals, Inclusions and Volcanic Processes

A Mineralogical Society of America Short Course

Organized and Edited by:
Keith Putirka, California State University Fresno
Frank Tepley, Oregon State University

Our use of minerals and their inclusions to understand magmatic systems has a long history, extending back to Sorby's (1858) study of inclusions and Darwin's (1844) and King's (1878) field studies of minerals. Although such work has been relatively continuous, notable advances by Barth (1934) and Roedder (1965) sparked interest in thermometry and inclusions respectively, and a series of papers by Eichelberger (1975), Anderson and Wright (1972), Anderson (1976) and Dungan and Rhodes (1978), among others, spurred new interest in using such methods to understand volcanic systems in particular. More recent advances in micro-analytical techniques over the past two decades, perhaps beginning with Davidson et al. (1990), have greatly magnified and accelerated interest in minerals and inclusions, highlighting the potential for scientific advancements and revised views of magma plumbing systems (Marsh, 1995). The short course and the related volume, 'Minerals, Inclusions and Volcanic Processes', was organized with the goal of summarizing where these earlier strands of research have now branched, with the added hope that such a review might initiate new collaborations, based on an alliance of complementary techniques. The prospects for such was perhaps indicated by the range in backgrounds and interests of the 207 people who registered for the short course, which was held on Dec. 13-14 in San Francisco. Here we present a summary of the 16 presentations (one for each chapter in the new volume).

Our first day began with a review by Julia Hammer on crystal kinetics and 'dynamic' experiments (where experimental *T* or *P* are not fixed), followed by a review of methods for estimating *P-T* conditions of crystallization. Hammer's review noted the importance of undercooling, not just to the formation of mineral textures, but also to its apparent requirement for the formation of melt inclusions. Her review also touched on observed decreases in crystal growth rates with time: even at a fixed difference between bulk liquidus *T* and experimental run *T*, the thermodynamic undercooling nevertheless decreases with time during an experiment (and in nature), due to crystal growth-driven changes in the composition of a magmatic system, as crystals and liquid approach equilibrium. This decrease in undercooling should decrease crystal growth rates, and so implies that true instantaneous growth rates are probably only captured in the earliest stages of a dynamic experiment. Keith Putirka followed with an analysis of mineral-melt-based thermometers and barometers, calibrated from static experiments (where *T* and *P* are fixed, in attempt to achieve equilibrium). He showed that to apply such models, natural systems must approach equilibrium. Tests for equilibrium usually rely on mineral-melt exchange coefficients that are expected to be independent of *T* and *P*, such as Fe-Mg exchange between olivine and liquid (Roedder and Emslie, 1970). Putirka showed that dynamic experiments can be used to test our 'tests of equilibrium' and that not all such tests provide a perfect filter. Where possible, multiple tests, (e.g., independent tests of equilibrium, or better, independent *P-T* estimates) can be crucial for narrowing uncertainty, and even then *P* estimates tend to be more precise when averaged. Lawford Anderson followed with a wide-ranging talk, showing applications of thermometers and barometers to granitic systems in the Sierra Nevada and the Transverse Ranges of California. In plutons from the latter, the Ti-in-zircon thermometer yields temperatures that are inversely correlated with Hf, with temperatures that range from just above the solidus to near the liquidus-and range to values that are higher than calculated for zircon saturation. This indication of a wide temperature range may be valid, but Anderson warned that the activities of trace components in minerals can be sensitive to modal mineralogy and liquid composition and that new experiments are needed to document such. The next talk, by Thor Hansteen and Andreas Klügel, reviewed methods to estimate pressures of fluid inclusions. Fluid inclusions have the potential for providing very precise *P* estimates, provided that inclusions are homogeneous, isochoric and remain closed ('Roedder's Rules'). Systems that violate these rules, though, can still be useful; Hansteen and Klügel presented frequency plots of *P* estimates, indicating how the peaks in such plots can be correlated to multiple depths of magma storage. A key limitation to the approach is the error associated with existing equations of state for fluids, which may not match natural fluid compositions, and are not derived from experiments conducted at high *P* and *T*. A promising result, however, is that fluid inclusions and mineral-melt equilibria, in some instances yield very similar pressure ranges.

Jon Blundy then presented work conducted in collaboration with Katherine Cashman, illustrating the utility of merging various petrologic approaches. They showed that at Mount St. Helens, mineral textures, melt inclusions and several different *P-T* estimation techniques yield an internally consistent picture of the depths and temperatures of partial crystallization and degassing rates at that volcano-a picture that is furthermore consistent with seismic studies that indicate depths of transport. Blundy also showed a *P-T* diagram illustrating calculated gradients in crystallinity and degree of volatile saturation, emphasizing that minerals within a single magma chamber may sample such variability and that *T* can be used as a proxy for proximity to a magma chamber wall. Malcolm Rutherford then presented a summary of methods for determining magma ascent rates from experimental investigations, and a survey of natural ascent rates. Rutherford showed that explosive magma ascent rates, as determined from amphibole-breakdown reactions, are similar to rates derived from decompression-induced crystallization (ca. 0.2 m/s for explosive ascent at Mount St. Helens), and both estimates are within an order of magnitude of estimates derived from seismicity (0.6 m/s at Mount St. Helens). Extrusive ascent rates are one to two orders of magnitude lower, and explosive ascent rates appear to be positively correlated with explosivity, indicating an important forensic role for petrology in the assessment of volcanic hazards.

We completed our first day with a review of volatile contents, and models used to estimate such. Nicole Métrich and Paul Wallace emphasized that to calculate the P of melt inclusion entrapment, the inclusion must be vapor saturated and there should be no post-entrapment volatile-loss, otherwise P estimates are systematically low. They also suggested that CO_2 loss (to shrinkage bubbles) can be significant. Wallace and Métrich noted, for example, that the highest pressures from olivine inclusions do not exceed 400 MPa and that fluid inclusions tend to yield higher pressures; they conclude that melt inclusions generally record simultaneous degassing and crystallization (as opposed to deep-seated storage). With these caveats, they showed that inclusions from a single eruptive unit can yield a range of saturation pressures; if magma ascent is the cause of degassing, this would seem to imply that inclusion capture is concurrent with magma rise. Their survey also showed that primitive phenocrysts tend to have higher CO_2 and H_2O contents, and that in some cases CO_2 fluxes may trigger H_2O loss, which in turn can trigger crystallization. They also showed that melt inclusion S contents are positively correlated with eruptive volume, and can be used to reconstruct volatile budgets for a given eruption

GN140 Content

correlated with eruptive volume, and can be used to reconstruct volatile budgets for a given eruption, with implications regarding climatic impacts. Gordon Moore concluded our first day with a summary of the characteristics of a good volatile solubility experiment, and tests of models that predict volatile contents or saturation pressures. Among the most important observations are that CO_2 and H_2O solubilities are highly sensitive to melt composition, which includes an interdependence of the two solubilities. Because of such sensitivities, saturation models should not be extrapolated outside the bounds of their calibration data. At present, only the models of Newman and Lowenstern (2002) (VolatileCalc) and Papale et al. (2006) account for compositional variations in mixed CO_2-H_2O-bearing melts. Both models appear to work well for rhyolites, while the Papale model appears to work better for more mafic systems, but has difficulties with Ca-rich basalts. For improvements to either model, new solubility experiments using mixed H_2O + CO_2 systems are critical.

Our second day began with an overview of melt inclusions, and continued with a discussion of isotopic studies. Adam Kent's review of melt inclusions emphasized both their benefits: they capture a wider range of complexity than revealed by whole rocks-and their pitfalls: they may record boundary layer melts, or melts that are otherwise not representative of macro-scale evolutionary processes. He and other presenters emphasized a plot by Faure and Schiano (2005) which shows how Ca/Al ratios can be used to differentiate whether melt inclusions have trapped far-field (i.e., representative) or near-field (non-representative compositions); Kent's survey showed that most inclusions appear to trap far-field compositions. Melt inclusions are also subject to re-equilibration, though their diversity indicates that magma transport rates greatly exceed the rates at which re-equilibration occurs. Frank Ramos and Frank Tepley followed with a summary of isotopic studies of mineral grains. The microsampling procedures they reviewed have been key in identifying potential equilibrium, and certain disequilibrium, between different grains and their host rocks and within individual crystals. Especially interesting are examples where individual crystals yield cores in disequilibrium and rims are in isotopic equilibrium with adjacent glass. Also, intergrain heterogeneity in some localities that has been thought to result from age differences, can in some instances be attributed to mixing between two components. Tepley and Ramos also illustrated some practical aspects of determining disequilibrium within and between crystals using both micromilling and laser ablation sample removal techniques, and low-blank chemical processing. Ilya Bindeman then followed with a survey of O isotope ratios from single crystals. Like their radiogenic counterparts, individual crystals yield a much wider range of O isotope ratios than their whole rock hosts, and much more heterogeneity than contained within bulk mineral separates. Among the more important results is that O isotopes provide a powerful tool for tracing the recycling of hydrothermally altered crust into magmatic systems. Oxygen also has an advantage of being slowly diffused compared to cations, and so O isotope heterogeneity can be preserved over longer times scales than other diffusing species. Our discussion of isotopes concluded with a review of crystal ages obtained from U-series disequilibria by Kari Cooper and Mary Reid. Cooper and Reid began their presentations with a discussion on how U-Th-Ra disequilibria are measured, plotted and interpreted in volcanic rocks. This led to a more in-depth discussion on each system (e.g., U-Th and Ra-Th disequilibria), including practical applications to volcanic systems. Their review of methods indicated that collection of such data is a highly time-intensive process, but with substantial rewards. For example, they showed that at Lacher See volcano in Germany, some flows yielded minerals with ages identical to (whole-rock derived) eruption ages, but that stratigraphically lower, more evolved whole rocks (presumably from the top of the magma chamber) hosted minerals that were 17 ka older than recorded by the whole rock system-perhaps representing material inherited from an earlier magmatic episode, and/or indicating the minimum subterranean life span for the nominally 12 ka Lacher See eruptive system. Cooper and Reid also showed U-series disequilibria at Mount St. Helens, which are suggestive of magma residence times on the order of decades to centuries.

The second day concluded with a series of talks related to diffusive time scales, mineral textures and physical models of magma extraction. Fidel Costa provided a detailed overview of the techniques used to obtain time-scales from diffusion profiles. Costa emphasized that diffusion profiles can yield times scales that are much shorter than can be accessed by radioisotope methods, and that the very young ages (compared to radioisotope methods) determined from diffusion profiles (mostly < 100y), reflect entrainment of older crystals and periods of crystal overgrowth-effectively re-equilibration, as opposed to the original time of crystal growth, as measured, for example, by U-series methods. Costa used the Bishop Tuff as an example, where diffusive time scales for Ti in quartz are very short (ca. 100 y) and likely reflect late stage re-heating and later crystal overgrowth, which may be especially important in large magmatic systems. As further evidence of such complexity, Martin Streck followed with a review and update of the textural observations that spurred the renewed interest in volcanic minerals more than 30 years ago. Like Bindeman, Streck emphasized that when individual crystals are viewed in detail, genetic terms as xenocryst and antecryst (older crystals from a related, but earlier magmatic episode) effectively lose their meaning. Individual crystals often record several episodes of growth and re-equilibration, and thus many phenocrysts (in the original sense of Iddings, simply a crystal that is conspicuous from groundmass or surrounding crystals) may have xenocryst cores, antecryst zones, and equilibrium rims, as the crystals are passed from one rock/magma to another. Streck showed how traditional methods of optical mineralogy, and other imaging methods, reveal different types of zoning, and that at Arenal, such textural studies of basaltic andesite lava flows allowed a precise enumeration of magmatic events (five) that contributed or affected the crystal population. The following discussion, however, indicated the discouraging trend that fewer students than ever are being trained to use a petrographic microscope.

Pietro Armienti followed Streck with a review of crystal size distributions (CSD) to estimate crystallization and magma transport rates. Armienti first showed that it is possible to derive the same CSD for a given sample regardless of the scale of sampling (which in the example from Mt. Etna range from a 7cm^2 thin section, to a photo covering >800 cm^2), provided one is careful with small- and large-end truncation effects. Armienti's review then showed that within a frequency plot of numbers of crystals vs. crystal length, the slope of the curve directly reflects the ratio of nucleation rate to growth rate, which should be constant when undercooling is constant. A key aspect of CSD then is that their slope directly reflects undercooling, and any changes in slope (at least in a closed system) can be interpreted as such. An interesting finding at Mt Etna is that CSD for rocks sampled near the vent are identical to those sampled downstream, indicating that crystallization occurred prior to eruption, not during downhill flow. Armienti also showed some potential new applications of CSD at Stromboli, where peaks in CSD may indicate degassing.

Our final talk by George Bergantz illustrated some of the latest work in attempting to understand physical mechanisms of magma storage and transport, especially as related to high-Si eruptions. Bergantz showed that many arc-related systems reveal a gap in SiO_2 among erupted products, an observation now named for Reginald Daly (Daly Gap), while others are strikingly homogeneous (monotonous intermediates of Hildreth, 1981). Bergantz showed how numerical studies indicate that convection, in different manifestations, can explain both suites. Sluggish convection can create or redistribute heterogeneities, as plumes move material from one part of a system to another, so producing thermal and chemical gradients, especially if the Reynolds number is low (Re<1, i.e., laminar flow). Even at high Re (>10^4, i.e., turbulent flow), heterogeneities can also be produced if convection is limited to a single overturn. Bergantz observes that monotonous intermediates preserve much microscopic-scale heterogeneity, and so reflect multiple overturn events, despite the fact that such flows tend to be rich in SiO_2 and crystal-rich, and so are viscous and resistant to forces that drive convection.

Although recent advancements initiated the organization of the short course and volume, the presentations and discussions that followed showed there is much work to be done. Undoubtedly, there remains a clear need to refine various tools through additional experiments, so as to better determine volatile saturation conditions and equations of state for complex fluids, as well as crystal kinetic parameters, and the development of mineral textures. The short course also highlighted that many current lines of investigation are highly complementary, and can be used to great effect in concert. For example, U-series ages appear to indicate the earliest stages of magma generation while diffusion profile ages inform us of the latest phases of transport. Similarly, mineral-melt barometers appear to inform us about the deeper parts of volcanic systems, and volatile-saturated equilibria inform us of the shallower-while fluid inclusions appear to record both, perhaps with higher precision. An alliance of methods can also provide key tests of our assumptions and interpretations. For example, if kinks in CSD are an indicator of degassing, then melt inclusions from related rocks with non-kinked CSD should yield higher volatile contents; if melt inclusions are being trapped largely upon upward transport, the times scales of such residence and transport, as might be inferred from diffusion profiles, should be consistent with transport times that might be inferred from a combination of ascent rate estimates from hornblende reaction-rims, and estimates of the depths from which magmas are delivered, as determined from geobarometers. To the extent that such tests yield a coherent picture of a volcanic system, the advances outlined at the short course and within the volume illustrate the promise of petrology and mineralogy for affording fundamental tests of the evolution of magma storage, transport and eruption.

Reference Cited

Anderson AT (1976) Magma mixing: petrological process and volcanological tool. J Volc Geoth Res 1:3-33.

Anderson AT, Wright TL (1972) Phenocrysts and glass inclusions and their bearing on oxidation and mixing of basaltic magmas, Kilauea volcano, Hawaii. Am Min 57:188-216.

Barth TW (1934) Temperatures in lavas and magmas and a new geologic thermometer. Naturen 6:187-192.

Darwin C (1844) Geological observations on the volcanic islands. London, Smith-Elder

Davidson, JP, DeSilva, SL, Holden, P, Halliday, AN (1990) Small-scale disequilibrium in a magmatic inclusion and its more silicic host. J Geophys Res 95:17661-17675

Dungan MA, Rhodes JM (1978) Residual glasses and melt inclusions in basalts from DSDP legs 45 and 46: evidence for magma mixing. Contr Min Petrol 67:417-431.

Eichelberger JC (1975) Origin of andesite and dacite: evidence of mixing at Glass Mountain in California and at other circum-Pacific volcanoes. Geol Soc Am Bull 86:1381-1391

Faure F, and Schiano P (2005) Experimental investigation of equilibration conditions during forsterite growth and melt inclusion formation. Earth Planet Sci Lett 236: 882-898

Hildreth W (1981) Gradients in silicic magma chambers: implications for lithospheric magmatism. J Geophys Res 86:10153-10192

King C (1878) Systematic Geology. U.S. Govt Print Office, Washington D.C.

Marsh BD (1995) Solidification fronts and magmatic evolution. Mineral Mag 60:5-40

Newman S, Lowenstern JB (2002) VolatileCalc: a silicate melt-H_2O-CO_2 solution model written in Visual Basic for Excel. Comp Geosci 28:597-604

Papale P, Moretti R, Barbato D (2006) The compositional dependence of the saturation surface of H_2O+CO_2 fluids in silicate melts. Chem Geol 229:78-95

Roedder, E (1965) Liquid CO_2 inclusions in olivine-bearing nodules and phenocrysts from basalts. Am Min 50:1746-1782

Sorby HC (1858) On the microscopic structures of crystals, indicating the origin of minerals and rocks. Geol Soc London Q J 14:453-500

Crossword - Polarized Light Microscopy

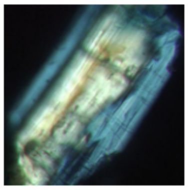

Glaucophane/crossite schist

Your friends at Geochemical News have created a microscopy-themed crossword.
Click the link to download the file:
GN140_Crossword_PLM.pdf [127KB PDF]

Need to check your answers? Here is the key:
GN140_Crossword_PLM-Key.pdf [315KB PDF]

Crossword puzzle references:
Phillips Revell Wm., 1971, Mineral optics. Freeman, San Francisco. 249 pp.
Wood, Elizabeth A., 1977, Crystals and Light. Dover, New York. 156 pp.

Crossword puzzle freeware:
EclipseCrossword 1.2.57. © 2000-2007 Green Eclipse. You may freely distribute crossword puzzles made with this software.
www.eclipsesoftware.com

GN140 Content

Polarized Light Microscopy

ACROSS

3. Areal proportions that are raised to the 3/2 power yield "___" proportions.
5. Angle of incidence equals angle of "___".
6. Quartz is a member of the "___" crystal system.
7. Point group of mineral barite.
10. 2V is the angle between "___" axes.
13. Uniaxial negative mineral; conoscopic illumination; optic axis perpendicular to microscope stage. You see an "___" figure.
19. Pink to green equals "___".
21. Uniaxial minerals viewed directly down the optic axis are "___".
24. Diminutive for Rebecca.
27. The distinction between glass and liquid is made solely on the basis of "___".
28. Filter above microscope stage that transmits light that vibrates only in an east-west direction.
32. Shape of indicatrix in cubic crystals.
33. Cools steam, yields water.
35. A crystal's optic angle [2V] is acute about the principal vibration direction Z. The crystal is said the be optically "___".
38. An aluminosilicate with chains of O-AL that are linked by the remaining Si, Al, and O ions. The optic axial plane is almost perpendicular to {100}, and is inclined at approximately 30° to {010}.
40. The Dodo bird was hunted to this end.
41. A type of equal-area stereonet.

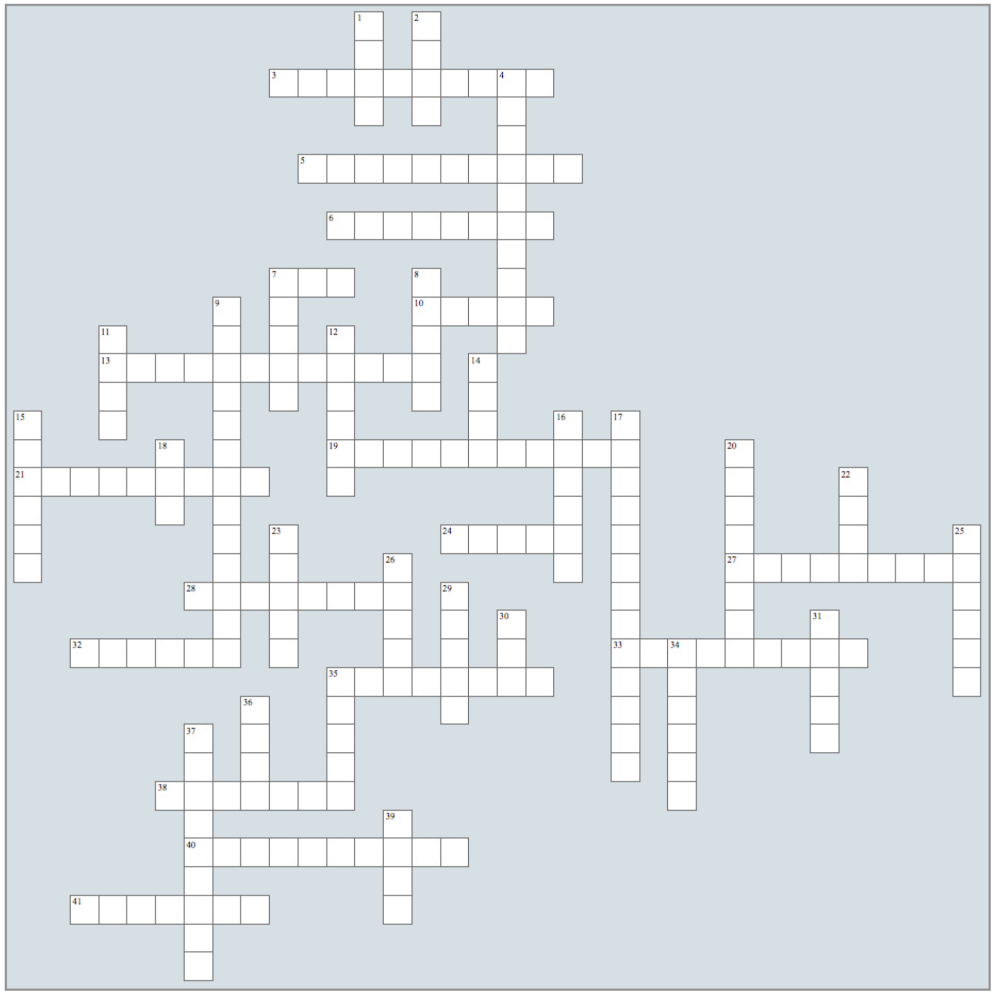

DOWN

1. "___" rotation axes are used in the most popular types of universal stage.
2. Point-counted modal proportions are percentages of "___".
4. In 1891, Fletcher proposed an "___", a purely imaginary geometric figure.
7. Molar formula weight divided by mineral weight equals number of "___".
8. As the plane of focus approaches the stage, the Becke line moves toward the substrate with "___" refractive index.
9. Wavelength affects the "___" only slightly.
11. Refractive indices of minerals composed of atoms with large atomic numbers are comparatively "___".
12. Volumetric proportions times densities yield "___" proportions.
14. Locate by orthoscopic illumination of uniaxial crystal.
15. Ideal thickness is of rock section for petrographic studies is "___" micrometers.
16. Equals the difference in refractive indices of a mineral and its surrounding medium.
17. Vibration and propagation directions of light in a mineral are always mutually "___".
18. Indicates that the microscope objective is strain free.
20. Felspars have perfect {001} "___".
22. Biaxial mineral, conoscopic light; vertical acute bisectrix; points of emergence of the two optix axes are sites of "___" retardation.
23. Universal stage measurements often are plotted on this type of stereonet.
25. Mineral in first-order red plate.
26. Remove the microscope's occular and place a uniaxial crystal between crossed polars. The interference figure is a "___".
29. German manufacturer of high-quality optics. Rhymes with bytes.
30. The last name of Roy's light spectrum.
31. German manufacturer of high-quality optics.
34. First name William; most microscopes have both upper and lower "___".
35. Optic "___" contains and is defined by the optic axes.
36. Two crystal individuals, on either side of a N-S or E-W reflection plane, that appear and extinguish sequentially on rotation of the polarizer.
37. The lenses of the common negative oculars are "___" oculars.
39. Mineral in ¼ λ plate.

Polarized Light Microscopy - Key